Biomaterials Science

ROYAL SOCIETY OF CHEMISTRY

PAPER

View Article Online
View Journal | View Issue

Cite this: *Biomater. Sci.*, 2025, **13**, 1426

Recyclable 3D printable single network granular hydrogels†

Gaia De Angelis, [a,b] Gaia Dupont,[a] Lorenzo Lucherini[a] and Esther Amstad *[a,b]

Received 1st July 2024,
Accepted 20th November 2024

DOI: 10.1039/d4bm00871e

rsc.li/biomaterials-science

Spherical microgels can be conveniently direct ink written into granular hydrogels because of their rheological properties when jammed. Yet, due to weak interparticle interactions, the resulting granular hydrogels are soft and often disassemble if immersed in aqueous media. These shortcomings can be addressed if microgels are firmly connected, for example through inter-particle covalent bonds or by introducing a second hydrogel network that interpenetrates the microgels and covalently connects them. However, these techniques typically hamper the recycling of the granular system. Here, electrostatic attraction forces between microgels and a polyelectrolyte are explored to directly print charged microgels into free standing structures in aqueous media. The resulting granular system remains stable in aqueous media for at least one month and can be recycled with minimal energy input.

Introduction

Hydrogels are soft materials characterized by crosslinked polymeric networks capable of retaining a high quantity of water. The composition of the polymer network and its structure determine the mechanical properties and functionality of the hydrogel, such that these assets can be varied over a wide range. The increasing demand for customised objects and hydrogels possessing locally varying compositions boosted the development of 3D printable hydrogels that can be used, for example, as biomimetic actuating systems,[1,2] especially in soft robotics.[3] For example, hydrogel-based soft robots that grip objects such as nails,[4] change their morphology upon exposure to external stimuli,[5] or mimic natural movements,[6] have been 3D printed. Most frequently, hydrogels possessing locally varying compositions are 3D printed through Direct Ink Writing (DIW). This technique enables local variations in compositions in all three dimensions with a spatial resolution of order 100 μm.[7] Yet, DIW imparts stringent rheological requirements such as shear thinning behaviour, fast stress recovery and a low yield stress to the inks.[8] Unfortunately, many hydrogel precursor solutions do not fulfil these requirements without the addition of rheomodifiers that risk to negatively impact the mechanical and sometimes optical properties of hydrogels. Hydrogels can be formulated as micrometre-sized microparticles, so-called microgels that, if jammed, display rheological properties, which are ideal for DIW. Granular hydrogels composed of spherical jammed microgels tend to be soft due to the weak inter-particle interactions that are often limited to frictional forces. Upon immersion in water, the inter-particle friction is further weakened, leading to the disassembly of these granular hydrogels. This limitation can be addressed by firmly connecting adjacent microgels through covalent bonds formed, for example, through enzymatic catalysis,[9] photo-initiated radical polymerization,[10] click chemistry,[11] and non-enzymatic amidation reactions.[12] However, these bonds typically result in stress concentrations that render the material brittle. Moreover, they hamper the recycling of the structure, an aspect that becomes increasingly important in the design of the next generation of polymer-based materials designed to minimally impact the environment.[13–15] Adjacent microgels can also be connected through physical interactions, including host–guest interactions,[16] electrostatic attraction,[17] hydrogen bonding,[18] and biotin–streptavidin conjugation.[19] Microgels formed through these interactions are self-healing, viscoelastic, and injectable. Cell-loaded microgels can additionally be connected through cell–cell interactions that yet, require time to form.[20] These structures can be actuated using external stimuli like fluidic, magnetic or acoustic forces. Yet, these structures can only be direct ink written at moderate resolutions and due to the reversible inter-particle interactions, they tend to collapse post-intervention.[21–23] Much stiffer granular hydrogels can be made by connecting microgels through a second hydrogel network.[24] Yet, the resulting double network granular hydrogels are difficult to recycle, or their recycling alters their mechanical properties.[25]

[a]*Soft Materials Laboratory, Institute of Materials, École Polytechnique Fédérale de Lausanne (EPFL), CH-1015 Lausanne, Switzerland. E-mail: esther.amstad@epfl.ch*
[b]*Bioinspired Materials National Center of Competence in Research (NCCR), Switzerland*

† Electronic supplementary information (ESI) available. See DOI: https://doi.org/10.1039/d4bm00871e

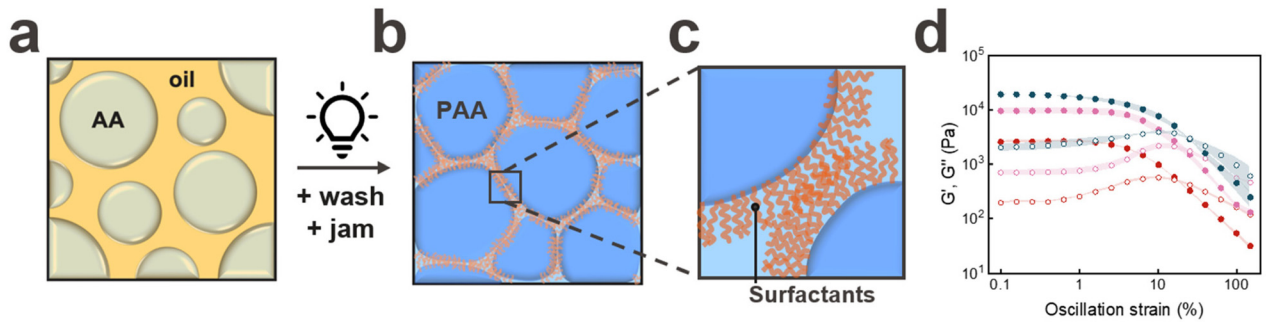

Fig. 1 Schematic illustration of the ink preparation, starting with (a) monomer loaded water in oil drops that are converted into microgels by (b) polymerising the acrylic acid (AA) within them through an UV light initiated free radical polymerization and jamming the resulting microgels to yield a 3D printable ink. (c) Close-up of microgels contained in granular hydrogels that are connected through hydrophobic interactions. (d) Storage (●) and loss (○) moduli of jammed microgels printed in air. Microgels are washed to remove the excessive surfactants (●). Minimally washed microgels containing Span80 (●) and Span20 (●) surfactants at their surfaces. Each experiment was repeated three times. The shaded area corresponds to the error bar calculated from three experiments.

Here, we introduce recyclable single network granular hydrogels that can be 3D printed in aqueous media and remain stable in these media for at least one month. This is achieved by exploiting electrostatic attraction forces between anionic microgels and a cationic polyelectrolyte that we use as a glue. Due to the electrostatic attraction between the microgels and the polyelectrolyte, the ink displays a spreading factor as low as 19% and the printed structure remains stable in aqueous media for at least one month. Due to the ability to reversibly break the inter-particle interactions, the printed granular structure can absorb a significant amount of energy even if immersed in water. We demonstrate that the 3D printed granular structures can be recycled in aqueous solutions under benign conditions within minutes. The Young's modulus of the recycled material decreases by only 22% after three iterations of recycling. Because of the self-healing properties and the recyclability, we consider this material to be well-suited for the next generation of recyclable underwater soft robotic systems.

Results and discussion

Granular hydrogels are typically soft because of weak inter-particle interactions that are often limited to inter-particle friction. To enhance inter-particle interactions without the need for labour- or cost-intensive post modification, we produce surface modified microgels in a single fabrication step by forming them from surfactant-stabilized water-in-oil emulsions, as schematically shown in Fig. 1a. Emulsions are converted into microgels by exposing them to UV light to initiate the free radical polymerisation reaction of the acrylic acid monomers contained in them, as shown in Fig. 1b.

To maintain the surface functionality of the microgels, we minimise the removal of surfactants from their surfaces during the washing cycles by only centrifuging the particles once. The presence of surfactants at the microgel surfaces is confirmed *via* Fourier Transform Infrared Spectroscopy (FTIR), as shown in Fig. S1a.†

To assess the suitability of jammed microgels to be 3D printed into self-supporting granular materials using DIW, we quantify the shear rate-dependent viscosity of jammed PAA microgels. As expected, the granular inks are shear thinning, as shown in Fig. S2.† Moreover, the pressure at the flow point, defined as the crossover of the storage G' and loss moduli G'', is in a range that is easily accessible with commercially available bioprinters, as shown in Fig. 1d. Similarly, the strain at the flow point is with 10% in a range that is well-suited for DIW, as shown in Fig. 1d.

To assess if the surface functionality of the microgels influences their rheological properties if jammed, we perform strain sweeps on them. Indeed, the plateau storage modulus of jammed microgels containing Span80 on their surfaces is significantly higher than that of jammed microgels that have been thoroughly washed to remove most of the surfactants from their surfaces, as shown in Fig. 1d. These results hint at the importance of the inter-particle hydrophobic interactions on the rheological properties of jammed microgels.

To assess the influence of the length of the hydrophobic chain on the inter-particle interactions, we stabilize the emulsion drops with Span20, which has a shorter hydrophobic chain with a molecular weight of 167 Da; this value is 50% lower than that of Span80.[26,27] The plateau storage modulus of jammed particles containing Span20 on their surfaces is significantly higher than that of counterparts surface modified with Span80, as shown in Fig. 1d. We assign this increase in G' to a denser polymer layer at the surfaces of microgels functionalised with Span20.

The degree of jamming of microgels strongly influences their rheological properties. To assess the robustness of our jamming protocol, we measure the rheological properties of unwashed PAA microgels that have been jammed through centrifugation and those that had additionally been put onto a filter paper to remove additional oil prior to their jamming. We do not observe any measurable influence of the additional

oil removal by the filter paper on the rheological properties of jammed PAA microgels, as shown in Fig. S1b.† By contrast the plateau storage and loss moduli of the paste significantly decrease if we only remove 80% of the oil or if we add 2 wt% lauryl acrylate to the oil, as shown in Fig. S1b.† These results demonstrate that our jamming protocol is robust. Yet, the rheological properties can be tuned through the addition of hydrophobic polymeric additives.

Our results suggest that inter-microgel interactions can be strongly increased by the surface functionalization of the microgels. Yet, the plateau storage moduli of our van der Waals forces reinforced granular materials are still very low, 17 ± 3 kPa. Van der Waals interactions are inherently weak. Stronger non-directional interactions include electrostatic interactions. To electrostatically reinforce granular hydrogels, we take advantage of the negative charge of PAA microgels dispersed in aqueous media at pH > 4.5 to reinforce them with a positively charged polyelectrolyte.

Polyelectrolyte-reinforced ink

To electrostatically reinforce the granular system, we add a positively charged crosslinker. To maximize the number of interaction sites between the microgels and the crosslinker, we employ a cationic polyelectrolyte, poly(diallyldimethylammonium chloride) (PD), as schematically shown in Fig. 2b and c. We inject jammed PAA microgels into an aqueous solution containing 1 wt% PD at pH = 7 and incubate the microgels for 24 hours. Indeed, the plateau storage modulus of PAA-based granular hydrogels reinforced with PD is 3.5-fold higher than that of granular hydrogels made of the same type of PAA microgels that have been 3D printed in air, as shown in Fig. 2d.

Due to the high molecular weight of PD, we expect it to only slowly diffuse into the interstitial spaces of the granular hydrogel. To assess if the soaking time influences G', we vary this parameter from 10 to 60 minutes. Within the tested range of soaking times, we do not observe any significant difference in G' of the reinforced granular hydrogels, as shown in Fig. 2d and Fig. S3b.† These results indicate that the inter-particle crosslinking through PD takes place within the first 10 minutes of incubation. To test if this suggestion is correct, we fluorescently label PD with fluorescein that is electrostatically attracted to it and visualise the structure with confocal microscopy. Fluorescein is preferentially localised at the microgel surfaces, as indicated in Fig. S4.† These results support our rheology data and suggest that PD is homogeneously distributed within the interstitial spaces even if samples are only incubated in a PD containing solution for 10 min. Hence, we keep the incubation time of the granular system in a PD containing solution constant at 10 minutes for the remainder of the experiments.

To assess the influence of the molecular weight of PD on the rheological properties of our electrostatically reinforced granular hydrogel, we vary the molecular weight of PD in the incubating solution from <100 kDa to 450 kDa. We do not see any significant change in the plateau G' if we change the PD molecular weight within the tested range, as shown in Fig. S5c.† Yet, the PD concentration influences the integrity of the granular hydrogel: if we increase the concentration of PD with a molecular weight of 250 kDa to 20 wt%, the granular hydrogels disassemble. We assign this result to the surface coverage of microgels with PD: if incubated in solutions containing high PD concentrations, we expect each microgel to be entirely surrounded by PD, resulting in positively charged microgels that electrostatically repel each other. To prevent this behavior, we fix the PD molecular weight to 250 kDa (medium) and the concentration within the incubating solution to 1 wt% for the remainder of this study.

Our results indicate that granular hydrogels composed of PAA microgels can be reinforced with an oppositely charged polyelectrolyte. To assess if we can reinforce these structures even more, we take advantage of the negatively charged groups

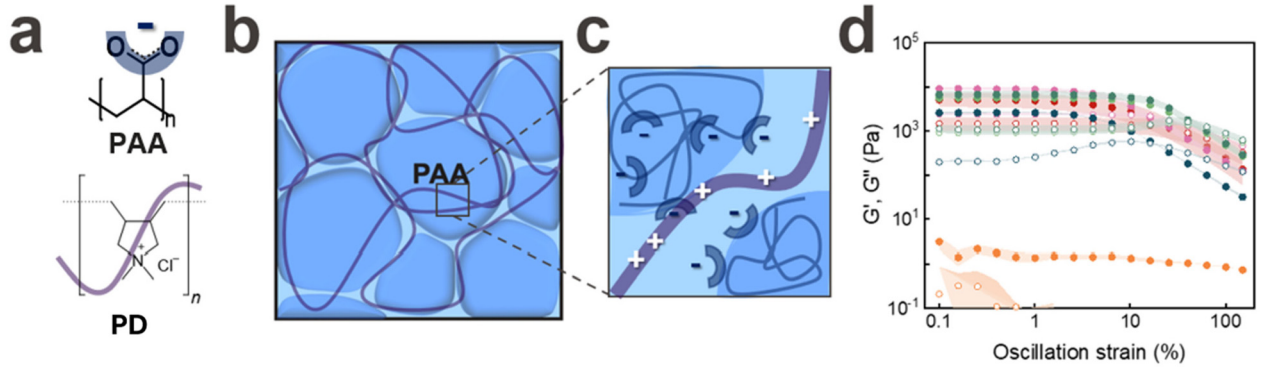

Fig. 2 Schematic illustration of interfacially reinforced granular hydrogels. (a) Chemical structure of (i) PD and (ii) a repeat unit of PAA with the respective schematic illustration. (b) Overview and (c) close-up of the inter-particle reinforcement through poly(diallyldimethylammonium chloride) (PD). Storage (●) and loss (○) moduli measured as (d) oscillation sweeps on jammed PAA microgels printed in air without any interfacial reinforcement (●) and samples that have been reinforced by incubating them in an aqueous solution containing PBS (●) and aqueous solutions containing 1 wt% PD for (●) 10 min, (●) 30 min, (●) 1 hour, and (●) 24 hours. All experiments have been repeated three times, shaded area corresponds to error bars.

from PAA to ionically crosslink them with di- and tri-valent ions. We print an ink composed of jammed PAA microgels into an aqueous bath containing Ca^{2+} ions. To ensure good solubility of all tested ions, we increase the pH of the incubating solution to 9. Structures that have been reinforced in the Ca^{2+} containing solution disassemble within 30 seconds, as shown in Fig. S6b(iv).† These results indicate that Ca^{2+} ions cannot efficiently connect adjacent microgels. To test if the ink dissolution is related to the weak Ca^{2+}-PAA interaction, we replace Ca^{2+} by Fe^{3+} because Fe^{3+} can ionically reinforce bulk PAA hydrogels.[28] Yet, granular hydrogels reinforced with Fe^{3+} also disassemble, as shown in Fig. S6b(v).† The disassembly of granular hydrogels might be related to the precipitation of Fe^{3+} ions that we observe within 5 minutes. To overcome this limitation, we replace Fe^{3+} with Cu^{2+}. However, we observe the same phenomenon where the structures disassemble, as shown in Fig. S6b(vi).† This observation suggests that ion-chelator pairs are insufficient to stabilize granular hydrogels composed of PAA microgels if immersed in aqueous solutions.

To strengthen our granular hydrogels, we 3D print structures in solutions containing a mixture of PD and ions, as shown in Fig. S6b(i–iii).† Indeed, these ion/polyelectrolyte reinforced structures remain stable. The storage plateau modulus of jammed PAA microgels crosslinked with PD and Cu^{2+} increases 9-fold compared to that of their non-ionically reinforced counterparts, up to 46 ± 2 kPa, as shown in Fig. 3c. Remarkably, granular hydrogels that are reinforced with PD and Cu^{2+} possess storage moduli that are two-fold higher than those of Fe^{3+} crosslinked counterparts and three-fold higher than those of their Ca^{2+} crosslinked counterparts. We assign the strong increase in G' to the orbital filling of Cu^{2+}: This ion has an electronic configuration of [Ar]3d9 and hence, a nearly complete d-shell. By contrast, Fe^{3+} has [Ar]3d5, signifying a half-filled d-shell, which imparts potential stability to the ion but reduced susceptibility to ionic crosslinking compared to Cu^{2+}, which lacks only one electron in its d-shell. This result highlights the importance of the ion-polyelectrolyte interactions for the storage modulus of granular hydrogels immersed in aqueous environments.

To assess the kinetics of the ionic crosslinking, we reduce the soaking time of the jammed PAA microgel in the PD and Cu^{2+}-containing solution from 24 h to 1 h. We do not observe any measurable influence of the soaking time on the plateau storage modulus, as shown in Fig. S6a.† These results indicate that the ionic crosslinking is completed within 1 h for structures with dimensions studied in this paper.

Direct ink writing (DIW)

To assess the filament spreading of the PAA based ink, we print it through a conical nozzle with a diameter of 410 μm into 30 × 30 × 1 mm^3 sized grids possessing an infill density of 15%. The spreading factor, determined as the percentage deviation from the programmed 3D printed square to the actual one, is as low as 15% if printed in air, as shown in Fig. 4d. The spreading factor increases by only 4% to 19% if we print the same ink into an aqueous solution containing 1 wt% PD, as shown in Fig. 4d. We attribute this very low spreading factor to the strong electrostatic attraction forces between PD and the microgels that enable the ink to quickly recover its solid-like

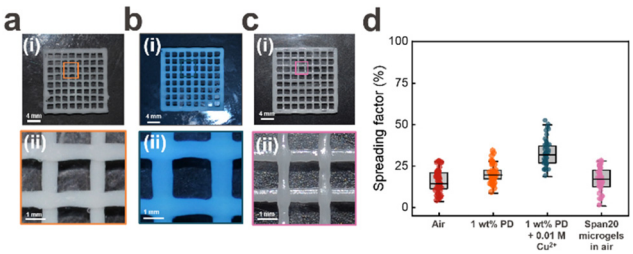

Fig. 4 Influence of interfacial reinforcement of granular hydrogels on the spreading factor: (i) overview and (ii) close-up photographs of meshes with side lengths of 3 cm that have been printed into an aqueous solution containing (a) 1 wt% PD and (b) 1 wt% PD + 0.01 M Cu^{2+} at pH 9 and (c) in air. (d) Summary of the spreading factor of jammed unmodified PAA microgels printed in air, unmodified microgels that have been printed into an aqueous solution containing 1 wt% PD and 1 wt% PD + 0.01 M Cu^{2+}, and microgels that contain Span20 at their surface.

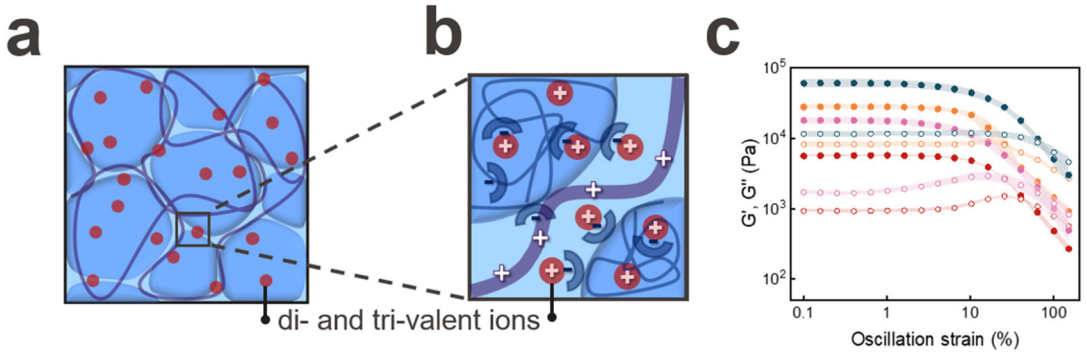

Fig. 3 (a) Overview and (b) close-up schematic illustration of granular hydrogels that are reinforced with PD and ions. (c) Oscillation strain measurements performed on jammed PAA microgels that have been 3D printed into an aqueous solution containing 1 wt% PD (●) and PD plus (●) Ca^{2+}, (●) Cu^{2+}, and (●) Fe^{3+} at a pH of 9. These samples have been soaked for 1 h. All experiments have been repeated three times, shaded area corresponds to error bars.

properties after the strain has been released. To test this attribution, we add 0.01 M Cu^{2+} ions to the incubation solution to weaken the electrostatic attraction forces. Indeed, this weakening of the inter-microgel interactions increases the spreading factor to 32%, as shown in Fig. 4b. If we remove PD from the incubating solution, the printed structure disassembles within 30 seconds, as shown in Fig. S3a(i)–(iv).† These results demonstrate the importance of the electrostatic inter-particle crosslinking on the spreading factor and stability of 3D printed granular hydrogels if submerged in aqueous media. Note that PAA microgels that have been surface modified with Span20 also disassemble if printed into aqueous solutions, as shown in Fig. S7.† These results indicate that the hydrophobic inter-microgel interactions are too weak to ensure the integrity of printed structures within aqueous solutions.

Stability in PBS

To test the stability of the PD reinforced granular hydrogels in the presence of salts that partially screen electrostatic interactions, we 3D print the EPFL logo and soak it in a PD containing aqueous solution for 10 min. We subsequently replace the PD-containing aqueous solution with Phosphate Buffered Saline (PBS). Remarkably, the structure retains its integrity for at least one month, which is the duration of the experiment, if stored at room temperature, as shown in Fig. 5c. We do not observe any change in the plateau storage modulus G' nor in any other rheological property we characterized after the structure has been incubated in PBS for one month, as shown in Fig. 5a and b. These results suggests that once PD electrostatically interacts with PAA microgels, it is strongly bound to their surfaces and does not partition into the surrounding solution even if it contains high concentrations of salts.

3D printing of free-standing structures

Our results indicate that PD efficiently electrostatically connects jammed PAA microgels such that they can be direct ink written at a high resolution. To assess if the inter-microgel connections are sufficiently strong to enable 3D printing of freestanding structures, we perform collapse tests on them.[29]

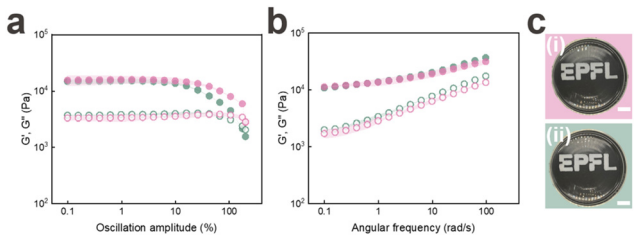

Fig. 5 Long-term stability of 3D printed electrostatically reinforced granular hydrogels. (a and b) Storage (●) and loss (○) moduli extracted from (a) oscillation and (b) shear rate sweeps of 3D printed structures that have been soaked in a PD containing aqueous solution for 10 min before being incubated in PBS of (●) 24 hours and (●) one month. Each experiment was repeated three times. (c) Photographs of 3D printed EPFL logos after they have been incubated in PBS for (i) 24 hours and (ii) 1 month. Scale bar 1.5 cm.

Remarkably, these electrostatically reinforced granular hydrogels do not significantly sag if printed over pillars with distances up to 16 mm, as shown in the photograph in Fig. 6a. These results suggest a yield stress of these materials of at least 542 Pa, as detailed in eqn (3) in the ESI.† We obtain similar results if we reinforce the granular hydrogels in an aqueous solution containing PD and Cu^{2+} ions, as shown in Fig. 6b. These results indicate the potential of our ink to print self-supporting free-standing structures.

Damping

Our ionically reinforced granular hydrogels possess a high density of attractive electrostatic interactions. As a result of these reversible bonds, the loss modulus G'' of this granular hydrogel is as high as 2000 ± 180 Pa, as shown in Fig. 3c. Hence, we expect this material to efficiently dissipate energy. To test this expectation, we 3D print a cube with a side length of 5 mm and reinforce it with PD. Indeed, this cube efficiently damps energy: if we drop a 1.1 g ball from a height of 10 cm onto the cube, the ball bounces back by only 1.9 cm, as shown in Fig. 7a. This result demonstrates that the cube absorbs 86 ± 4% of the potential energy of the impacting ball, as shown in Fig. 7a. The cube damps the impact of the ball even more efficiently if it is reinforced with PD and Cu^{2+}. If dropped onto these cubes, the ball bounces back to only 1.8 cm, as shown in Fig. 7b. These results indicate that the Cu^{2+}-reinforced granular PAA absorbs 90 ± 5% of the potential energy of the impacting ball, as shown in Fig. 7b. In contrast, water absorbs only 40 ± 2% of the potential energy: when the ball is dropped into a Petri dish filled with water, it bounces back to a height of 2.5 cm, as shown in Fig. S8.† Similarly, when dropped onto a bulk PAA cube submerged in water, it only absorbs 62 ± 3% of the energy, as shown in Fig. S9.† This comparison highlights the benefit if the granular structure for energy dissipation. This feature sets apart our microgel system from traditional single-network granular hydrogels, which disassemble if

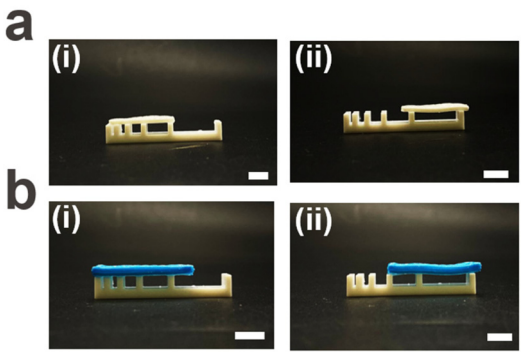

Fig. 6 Mechanical stability of PD-reinforced granular hydrogels. Photographs depicting a rectangle with dimensions of 3 × 1 × 0.1 cm^3 composed of jammed PAA microgels 3D printed onto a Teflon support that has been immersed in an aqueous solution containing (a) 1 wt% PD and (b) 1 wt% PD + 0.01 M Cu^{2+} at pH 7 for 12 hours. The rectangle does not measurably sag if put on top of pillars separated by (i) 1.0, 2.0, 4.0, 8.0, and (ii) 16.0 mm. The scale bars are 8 mm.

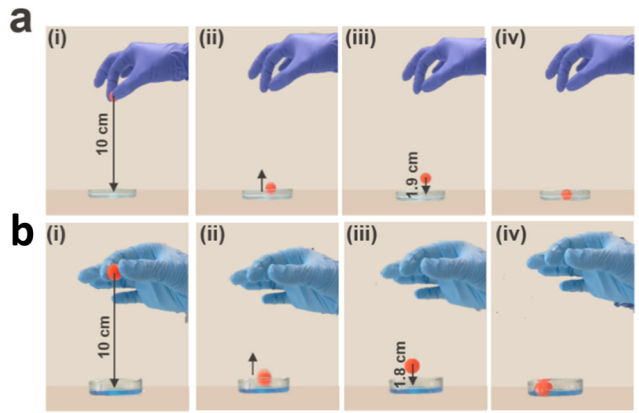

Fig. 7 Electrostatically reinforced granular hydrogels as underwater dampers. (a and b) Time-lapse photographs of a 3D printed cube with side lengths of 5 mm composed of jammed PAA microgels that have been incubated in an aqueous solution containing (a) 1 wt% PD and (b) 1 wt% PD + 0.01 M Cu^{2+}. A ball composed of polyethylene terephthalate glycol (PETG) with a diameter of 1.4 cm is dropped from a height of 10 cm onto the square.

immersed in aqueous solutions, as shown in Fig. 2d and Fig. S4b.†

Degradation and recycling

The rapidly increasing urge to recycle polymer-based materials demands new energy-efficient and benign strategies. We consider our granular system to be predestined for recycling as it can be decomposed into microgels that can readily be recovered at high yields through sedimentation without the need to break any covalent bonds. We expect our granular system to disassemble into microgels and polyelectrolytes under benign aqueous conditions and to be recycled into granular materials possessing identical mechanical properties. To test our expectation, we 3D print the red part of the Swiss flag and reinforce it with PD, as shown in Fig. 8a(i). We immerse the self-standing granular hydrogel into an aqueous solution containing 1 M bicarbonate, whose pH is 9. The acidic proton (H^+) from the carboxylic acid of PAA interacts with the bicarbonate ion (HCO_3^-) to form carbonic acid (H_2CO_3) and the sodium salt of the carboxylic acid (R-COONa). Carbonic acid (H_2CO_3) is unstable in aqueous media leading to its decomposition into water (H_2O) and carbon dioxide gas (CO_2).[30] Indeed, within 10 minutes, bubbles, indicative of CO_2, form and the structure starts to disassemble, as shown in Fig. 8a(ii). We attribute this phenomenon to the carboxylic acid groups of PAA that, upon their complexation with Na^+, no longer electrostatically attract PD. We recover 78 ± 3% of the microgels by centrifugation. These microgels can be jammed and 3D printed into the white part of the Swiss flag, as shown in Fig. 8a(iii). We measure a decrease in the storage modulus of the recycled granular hydrogel of only 22% after 3 cycles, as shown in Fig. 8b. We attribute this loss to some PD polymers that are electrostatically attracted by the surface of one microgel only, such that they do not bridge adjacent microgels anymore. This result points to the potential of our material to be used as 3D printable and recyclable underwater dampers, which reduces waste and lowers long-term costs associated with material production in underwater environments.

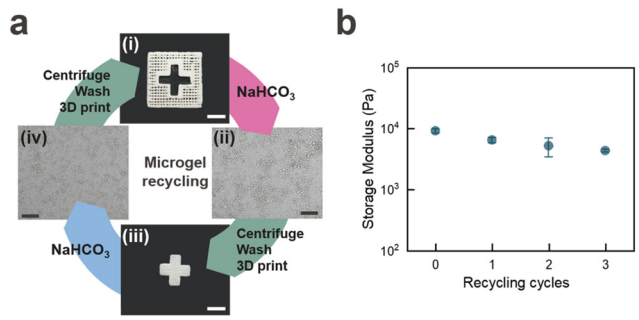

Fig. 8 (a) Recycling of electrostatically reinforced granular hydrogels. (a) Overview of the recycling of (i) jammed PAA microgels that have been 3D printed into a Swiss flag before being reinforced with PD. (ii) The structure decomposes if immersed in an aqueous solution containing 1 M sodium bicarbonate ($NaHCO_3$), resulting in individually dispersed microgels. (iii) The microgels are washed, jammed and 3D printed into a white cross before being reinforced with PD. (iv) The cross disassembles by immersing it in an aqueous solution containing 1 M $NaHCO_3$ to yield dispersed microgels that can again be washed, jammed, and 3D printed. Each experiment was repeated three times. Scale bars for (i) and (iii) are 1 cm, whereas for (ii) and (iv) they are 200 μm. (b) Influence of the number of recycles the granular hydrogel has been subjected to on the plateau storage modulus.

Conclusions

We introduce recyclable single network granular hydrogels that possess high loss moduli in aqueous solutions such that they can be used as excellent underwater dampers. The hydrogels are composed of poly(acrylic acid) (PAA) microgels that are electrostatically crosslinked with poly(diallyldimethylammonium chloride) (PD) and optionally ionically reinforced with Cu^{2+}. The electrostatic inter-particle interactions enable 3D printing of cm-sized free-standing structures that remain stable for at least one month even if incubated in a physiologic buffer such as PBS. The unique combination of electrostatic interactions and ionic reinforcement opens new possibilities for the 3D printing of cm-sized free-standing structures that we envisage to be well-suited self-healing underwater dampers and actuators.

Materials and methods

Acrylic acid (AA), sodium bicarbonate powder ($NaHCO_3$), mineral oil light, phosphate-buffered saline (PBS), copper(II) chloride dihydrate, polydiallyldimethylammonium chloride (PD) low/medium/high molecular weight, 2-hydroxy-2-methylpropiophenone (PI) (Sigma-Aldrich), *N*,*N*′-methylebenbisacrylamide (MBAA), calcium chloride (Carl Roth), iron

(III) chloride hexahydrate (Acros Organics), ethanol absolute, 99.8% (ThermoFisher), sorbitan monolaurate (Span20) (ABCR Chemicals), ABIL EM 90 modified polyether-polysiloxane (Evonik), and Span80 (TCI Chemicals), are used as received.

Microgel preparation. We use deionized water containing 30 wt% AA, 7.5 wt% (with respect to the monomer) MBAA, and 5 μL mL^{-1} PI as the dispersed phase and mineral oil containing either 2 wt% ABIL-EM90, 2 wt% Span80, or 2 wt% Span20 as the continuous phase. The two phases are mixed at a volume ratio of 6 : 1 oil to water, and vortexed to emulsify. To convert drops into microgels, the drops are exposed to UV light (UWAVE, UCUBE-365-100) for 5 minutes at 36% intensity. The resulting PAA microgels are transferred into ethanol and centrifuged at 4500 rpm for 10 minutes (Mega Star 1.6R, VWR) to eliminate the oil. The supernatant is discarded, unless otherwise specified. This process is repeated three times with ethanol and three times with water. The purified PAA microgels are resuspended in water for storage.

3D printing. Individually dispersed PAA microgels are converted into an ink by jamming them, which is achieved by centrifuging the microgels at 4500 rpm for 10 minutes.[24] The resulting microgel ink is loaded into a 3 mL Luer lock syringe. To eliminate trapped air, the syringe is sealed and centrifuged at 4500 rpm for 2 minutes. The microgels are 3D printed using a commercial 3D bioprinter (Inkredible+, Cellink) and extruded through a conical nozzle with a diameter of 410 μm, driven by a pressure-controlled piston at 55 kPa, with a printing speed of 10 mm s^{-1}. Printing is carried out either on an empty Petri dish or within a Petri dish containing the appropriate aqueous solution, with an initial gap of 0.1 mm. For samples that are used in rheological measurements, a high infill density is used to avoid any gaps in the structure.

Rheological measurements. The rheological properties of the granular hydrogels are measured using a DHR-3 TA Instrument featuring an 8 mm diameter plate–plate steel geometry. Oscillation sweeps are performed at room temperature with a frequency of 10 rad per s. Frequency sweep measurements are performed at room temperature with an oscillation strain of 1%. Before starting the measurements, the samples are relaxed for 60 seconds, and the gap is set to 800 μm. The excess material that is pushed out from the sides of the geometry is carefully removed, ensuring that the rheometer only analyses the material between the plate and the geometry. Mineral oil is applied around the samples to prevent them from drying.

Spreading factor. The granular ink is printed as a grid (30 × 30 × 1 mm^3) with an infill density of 15%. The spreading coefficient is calculated using eqn (1):

$$\text{Spreading factor}\,(\%) = \frac{A_P - A_T}{A_T} \times 100 \quad (1)$$

where A_P is the area measured from optical microscopy images, and A_T is the theoretical area of a printed square.

Energy damping. The damping energy of our granular hydrogel is quantified on 3D-printed cubes with a side length of 5 mm. These cubes are immersed in an aqueous solution containing either 1 wt% PD or a combination of 1 wt% PD and 0.01 M Cu^{2+} for 12 hours. The samples are removed and a sphere made of polyethylene terephthalate glycol (PETG) with a diameter of 1.4 cm and a weight of 1.1 g is dropped from a height of 10 cm onto it, while the entire process is recorded at 60 fps (iPhone 14 Pro, Apple). The potential energy before dropping the ball and after the first bounce is calculated as:

$$E_p(J) = mgh \quad (2)$$

where m is the mass of the ball in kg, g is the gravitational force in N kg^{-1}, and h is the height in meters from where the ball falls. The potential energy absorbed by the material is determined by calculating the difference between the initial potential energy and the potential energy after the first bounce.

Degradation and recycling of microgels. Granular hydrogels are decomposed by pouring an aqueous solution containing 1 M $NaHCO_3$ in the Petri dish containing the 3D printed samples. The Petri dish is agitated manually to facilitate the dispersion of microgels. The dispersed microgels are recovered through centrifugation at 4500 rpm for 10 minutes (Mega Star 1.6R, VWR). The retrieved particles are subjected to multiple washing cycles in excess water and centrifuged until the pH of the supernatant reaches 6. This washing process is repeated three times to ensure thorough cleaning. The cleaned microgels are jammed and further used for the 3D printing of additional structures.

Filament collapse tests. A platform featuring pillars with dimensions of 2.0 × 2.0 × 4.0 mm^3 is used. These pillars are positioned at gap distances of 1.0, 2.0, 4.0, 8.0, and 16.0 mm from each other.[29] A 3D-printed rectangle measuring 30 × 30 × 1 mm^3 is soaked for 12 hours in an aqueous bath containing either 1 wt% PD or 1 wt% PD + 0.01 M Cu^{2+}. The rectangle is carefully transferred onto the pillar-supported platform and imaged (iPhone 14 Pro, Apple). The yield stress is calculated using eqn (3):

$$\sigma_{stress} = \frac{\rho \times g \times L}{\sin\theta} \quad (3)$$

where ρ is the density of the material, g is the gravitational acceleration, which we approximate as 9.81 ms^{-2}, L is the distance from the edge of the pillar to the midpoint of the suspended rectangle, and θ the angle of deflection of the rectangle with the horizontal direction.

Fluorescence confocal microscopy. We perform fluorescence confocal microscopy using a Leica SP8 STED 3X with an excitation wavelength 489 nm. The wavelength is recorded between 500 and 550 nm. The objective is 25×, water immersion with NA 0.75.

Author contributions

G. De Angelis and E. Amstad designed the experiments. G. De Angelis performed the printability, energy damping, recyclabil-

ity, and filament collapse experiments. G. Dupont performed all rheology and stability experiments. L. Lucherini performed the confocal microscopy experiments and offered intellectual contribution for the application side of this work. G. De Angelis and G. Dupont performed the rest of the experiments together. G. De Angelis, G. Dupont, and E. Amstad analysed the data and wrote the manuscript.

Data availability

The data supporting this work is available on request from the corresponding author, EA.

Conflicts of interest

There are no conflicts to declare.

Acknowledgements

The authors would like to thank all the members of the Soft Materials Laboratory (SMaL) for fruitful discussions, especially Eva Baur for her help with the energy damping experiments, and Francesca Bono and Tianyu Yuan for their help on the filament collapse tests. We thank the BioImaging and Optics Core facility (BIOP) at EPFL, where we performed the fluorescence confocal microscopy experiments. The work was financially supported by the bioinspired materials NCCR (205603).

References

1 A. K. Mishra, W. Pan, E. P. Giannelis, R. F. Shepherd and T. J. Wallin, *Nat. Protoc.*, 2021, **16**(4), 2068–2087.
2 X. Le, W. Lu, J. Zhang and T. Chen, *Adv. Sci.*, 2019, **6**(5), 1801584.
3 Y. Cheng, *et al.*, *ACS Nano*, 2019, **13**(11), 13176–13184.
4 L. Yang, J. Miao, G. Li, H. Ren, T. Zhang, D. Guo, Y. Tang, W. Shang and Y. Shen, *ACS Appl. Polym. Mater.*, 2022, **4**(8), 5431–5440.
5 A. Mateescu, Y. Wang, J. Dostalek and U. Jonas, *Membranes*, 2012, **2**(1), 40–69.
6 J. Choi, D. Lee and J. Hyun, *Cellulose*, 2022, **29**, 2351–2369.
7 M. Tang, Z. Zhong and C. Ke, *Chem. Soc. Rev.*, 2023, **52**, 1614–1649.
8 J. A. Lewis, *Adv. Funct. Mater.*, 2006, **16**(17), 2193–2204.
9 D. R. Griffin, W. M. Weaver, P. O. Scumpia, D. Di Carlo and T. Segura, *Nat. Mater.*, 2001, **14**(7), 737–744.
10 A. Sheikhi, J. de Rutte, R. Haghniaz, O. Akouissi, A. Sohrabi, D. Di Carlo and A. Khademhosseini, *Biomaterials*, 2019, **192**, 560–568.
11 A. S. Caldwell, G. T. Campbell, K. M. T. Shekiro and K. S. Anseth, *Adv. Healthcare Mater.*, 2017, **6**(15), 1700254.
12 F. Li, V. X. Truong, P. Fisch, C. Levinson, V. Glattauer, M. Zenobi-Wong, H. Thissen, J. S. Forsythe and J. E. Frith, *Acta Biomater.*, 2018, **77**, 48–62.
13 G. Chyr and J. M. DeSimone, *Green Chem.*, 2023, **25**(2), 453–466.
14 S. Kolluru, A. Thakur, D. Tamakuwala, V. V. Kumar, S. Ramakrishna and S. Chandran, *Polym. Bull.*, 2024, **81**, 9569–9610.
15 S. A. Miller, *ACS Macro Lett.*, 2013, **2**(6), 550–554.
16 A. Harada, R. Kobayashi, Y. Takashima, A. Hashidzume and H. Yamaguchi, *Nat. Chem.*, 2011, **3**, 1.
17 Y. L. Han, *et al.*, *Biofabrication*, 2013, **5**(3), 035004.
18 C. Y. Li, D. K. Wood, C. M. Hsu and S. N. Bhatia, *Lab Chip*, 2011, **11**(17), 2967–2975.
19 Y. Hu, A. S. Mao, R. M. Desai, H. Wang, D. A. Weitz and D. J. Mooney, *Lab Chip*, 2017, **17**(14), 2481–2490.
20 Y. T. Matsunaga, Y. Morimoto and S. Takeuchi, *Adv. Mater.*, 2011, **23**(12), H90–H94.
21 S. E. Chung, W. Park, S. Shin, S. A. Lee and S. Kwon, *Nat. Mater.*, 2008, **7**(7), 581–587.
22 Y. Du, E. Lo, S. Ali and A. Khademhosseini, *Proc. Natl. Acad. Sci. U. S. A.*, 2008, **105**(28), 9522–9527.
23 S. Tasoglu, C. H. Yu, H. I. Gungordu, S. Guven, T. Vural and U. Demirci, *Nat. Commun.*, 2014, **5**(1), 4702.
24 M. Hirsch, A. Charlet and E. Amstad, *Adv. Funct. Mater.*, 2020, **31**(5), 2005929.
25 A. Charlet, M. Hirsch, S. Schreiber and E. Amstad, *Small*, 2022, **18**(12), 2107128.
26 'Span 20 1338-39-2'. Accessed: Jan. 19, 2024. [Online]. Available: **https://www.sigmaaldrich.com/**.
27 'Span 80 Sigma CAS No.1338-43-8'. Accessed: Jan. 19, 2024. [Online]. Available: **https://www.sigmaaldrich.com/**.
28 M. Hirsch, L. D'Onofrio, Q. Guan, J. Hughes and E. Amstad, *Chem. Eng. J.*, 2023, **473**, 145433.
29 A. Ribeiro, *et al.*, *Biofabrication*, 2017, **10**(1), 014102.
30 'Sodium bicarbonate test – Labster'. Accessed: Jan. 19, 2024. [Online]. Available: **https://theory.labster.com/sodiumbi_test/**.